

Probing exciton-phonon interaction in AlN epilayers by photoluminescence

A. Sedhain, J. Li, J. Y. Lin, and H. X. Jiang^{a)}

Department of Electrical and Computer Engineering, Texas Tech University, Lubbock, Texas 79409, USA

(Received 2 May 2009; accepted 28 July 2009; published online 14 August 2009)

Deep ultraviolet (DUV) photoluminescence (PL) spectroscopy has been employed to investigate the exciton-phonon interaction in AlN. Longitudinal optical (LO) phonon replicas of free exciton recombination lines were observed in PL emission spectra, revealing the coupling of excitons with LO phonons. We have quantified such interaction by measuring Huang–Rhys factor based on polarization resolved DUV PL measurements. It was observed that the exciton-phonon coupling strength in AlN depends on the polarization configuration and is much larger in the direction with the electrical field (\vec{E}) of the emitted light perpendicular to the wurtzite c -axis ($\vec{E} \perp \vec{c}$) than in the direction of $\vec{E} \parallel \vec{c}$. Furthermore, a larger coupling constant was also measured in AlN than in GaN. The large effective hole to electron mass ratio in AlN, especially in the $\vec{E} \perp \vec{c}$ configuration, mainly accounts for the observed results. © 2009 American Institute of Physics. [DOI: 10.1063/1.3206672]

AlN has attracted tremendous interest as a semiconductor material for deep UV (DUV) optoelectronic device applications because of its ultrahigh direct bandgap (~ 6.1 eV). Recent advances in epitaxial growth techniques have made it possible to grow high quality AlN epilayers on different substrates.^{1–5} A few active DUV devices based on pure AlN have also been demonstrated, including light emitting diodes with an emission wavelength of 210 nm (Ref. 6) and metal-semiconductor-metal and Schottky barrier photodetectors for DUV and extreme UV device applications.^{7–9} The availability of device quality AlN epilayers also opens up new opportunities for probing fundamental parameters in AlN to a degree previously unattainable. Due to the ionic nature of III-nitrides, Frohlich interaction, which is the Coulomb interaction between electrons (holes) and longitudinal electric field produced by the zone-center longitudinal optical (LO) phonons, is stronger compared to deformation-potential or piezoelectric interaction in these materials. The coupling of carriers with LO phonons strongly influences the optical and transport properties of III-nitrides.¹⁰

The A_1 (LO) phonon in AlN has an energy of about 110 meV as determined by the Raman spectroscopy measurement.¹¹ There have been previous reports on carrier-phonon interaction in GaN,^{12,13} InGaN/GaN, and GaN/AlGaN quantum wells.¹⁴ To the best of our knowledge, no experimental work has been reported on the strength of such interactions in AlN due to the lack of high quality materials and proper characterization tools to match the ultrahigh band gap of AlN in the past. In this letter, we report on the observation of phonon replicas associated with the free exciton recombination and polarization resolved photoluminescence (PL) measurement of the exciton-phonon coupling strength (S) in wurtzite AlN.

AlN homo- and heteroepilayers with thicknesses of about 0.5 μm were synthesized by metal organic chemical vapor deposition on both (0001) sapphire (Al_2O_3) and AlN bulk crystal substrates (supplied by Crystal IS, Inc.). A thin layer of AlN buffer was deposited at 550 °C prior to the growth of the heteroepilayer. Trimethyl aluminum and am-

monia (NH_3) were used as Al and nitrogen sources. AlN epilayers were grown at 1200 °C with a V/III ratio of around 150. PL signals were collected in two different configurations of the polarization of emitted light, e.g., the electrical field of the PL emission is directed either parallel ($\vec{E} \parallel \vec{c}$) or perpendicular ($\vec{E} \perp \vec{c}$) to the wurtzite c -axis. A frequency quadrupled Ti-sapphire laser with a repetition rate of 76 MHz and 100 fs pulse width operating at 197 nm was focused onto the sample surface through a microscope objective. The collected PL signal was then dispersed by a 1.3 m monochromator and detected by a microchannel-plate photomultiplier tube.

Low temperature (10 K) PL spectra of an AlN epilayer grown on c -plane sapphire are shown in Fig. 1 for both $\vec{E} \parallel \vec{c}$ and $\vec{E} \perp \vec{c}$ configurations. The PL spectrum collected in the $\vec{E} \parallel \vec{c}$ configuration shown in Fig. 1(a) exhibits the main free exciton emission line at 6.06 eV (Ref. 15) and two weaker peaks at 5.95 and 5.84 eV. The energy separation between

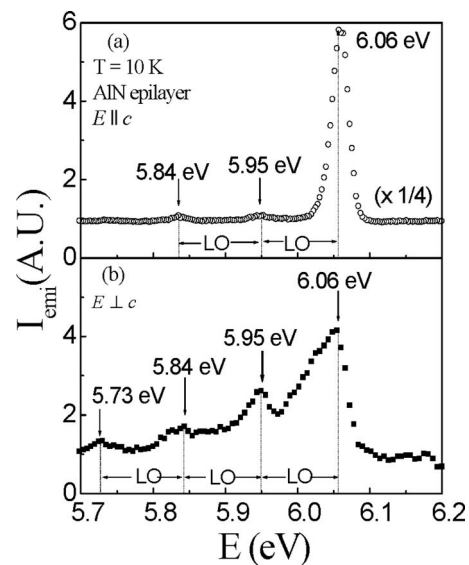


FIG. 1. Low temperature (10 K) PL spectra of an AlN heteroepilayer collected with the polarization of emitted light (a) parallel ($\vec{E} \parallel \vec{c}$) and (b) perpendicular ($\vec{E} \perp \vec{c}$) to the crystallographic c -axis.

^{a)}Electronic mail: hx.jiang@ttu.edu.

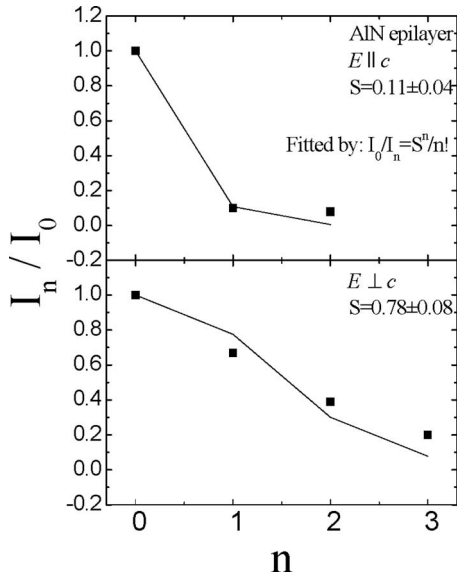


FIG. 2. Normalized PL intensities of n th order phonon replicas with respect to the zero phonon line measured in an AlN heteroepilayer in two different polarization configurations.

the successive emission lines is 110 meV, which corresponds to the value of the LO phonon energy in AlN.¹¹ We thus assign the two lower energy peaks to the $n=1$ and $n=2$ phonon replicas of the main exciton transition line ($n=0$) in order by decreasing energy. We observed a similar trend of phonon assisted excitonic emission in the $\vec{E} \perp \vec{c}$ configuration, as illustrated in Fig. 1(b). In the latter case, though the intensity of the main exciton emission line ($n=0$) is much lower than that in the $\vec{E} \parallel \vec{c}$ configuration due to the unique fundamental band structure of AlN,¹⁶ the relative intensities of phonon assisted emission lines are much higher and LO phonon replicas up to $n=3$ have been resolved. The appearance of the phonon replica lines is a clear indicator of a strong carrier-phonon interaction in AlN. It is also noted that the observed phonon lines have an energy separation corresponding to the A_1 (LO) phonon in AlN (110 meV) and no other phonon replica lines have been observed. This is consistent with the fact that the electron-LO phonon Frohlich interaction is the strongest in AlN.¹⁰

The distribution of emission intensities among the main peak ($n=0$) and the phonon replicas ($n=1$ and $n=2$) depends on the exciton-phonon coupling strength, which is expressed by Huang–Rhys factor S within the Franck–Condon approximation. At low temperatures, the emission intensity of the n th phonon replica (I_n) and the main emission line (I_0) are related by^{17–19}

$$I_n = I_0(S^n/n!), \quad (1)$$

where $n=0,1,2,3,\dots$, which represent the number of LO phonons involved.

Figure 2 plots I_n/I_0 for both $\vec{E} \parallel \vec{c}$ and $\vec{E} \perp \vec{c}$ configurations. It is interesting to note that the coupling constant, S , in AlN varies greatly between the two polarization configurations of emitted light. The S -parameter obtained by fitting the observed I_n/I_0 with Eq. (1) is $S^\perp = 0.78$ in the $\vec{E} \perp \vec{c}$ configuration, which is much higher than the value of $S^\parallel = 0.11$ measured in the $\vec{E} \parallel \vec{c}$ configuration.

For the free exciton in materials with wurtzite structures, the exciton-phonon coupling constant may be expressed in

terms of the fundamental quantities including optical and static dielectric constants (k_o, k_s), the hole to electron effective mass ratio ($\alpha = m_h/m_e$), Bohr radii of electron and hole (a_e, a_h), and LO phonon energy $\hbar\omega_{LO}$ ($=110$ meV) as follows:²⁰

$$S = \frac{5}{16} \frac{e^2}{\hbar\omega_{LO}} \left(\frac{1}{k_o} - \frac{1}{k_s} \right) \left[\frac{1}{a_h} + \frac{1}{a_e} - \frac{16(\alpha^2 + 3\alpha + 1)}{5a_e(\alpha + 1)^3} \right]. \quad (2)$$

It can be seen that between the two polarization configurations in AlN, the difference in the coupling parameter (S) predominantly originates from the value of α since a_h and a_e are also related with α through the relationship of $a_{h(e)} = a_{ex}/(1 + m_{h(e)}/m_{e(h)})$, where $a_{ex} = (1/m_h + 1/m_e)m_0k_s a_0$ (Ref. 21) is the ground state exciton Bohr radius. More specifically, the value of α is about 42 in the $\vec{E} \perp \vec{c}$ configuration and is about 11 in the $\vec{E} \parallel \vec{c}$ configuration.²² We have attempted to utilize Eq. (2) to estimate the hole effective mass anisotropy from the measured S values of $\vec{E} \perp \vec{c}$ and $\vec{E} \parallel \vec{c}$ configurations. The deduced value of m_h^\perp/m_h^\parallel from the measured S^\perp and S^\parallel is about a factor of 2 larger than the calculated value, which is about 3.2.²² We thus believe that Eq. (2) is able to provide a qualitative explanation to the measured S values. However, it has to be cautioned to use it to explain experimental results quantitatively.

The measured S -parameters in AlN in both polarization configurations are much larger than a previously reported value of about 0.007 in GaN epilayers in which the PL emission is polarized predominantly in the $\vec{E} \perp \vec{c}$ configuration.²³ In addition to possible differences in material qualities, several factors may also account for this enhanced coupling in AlN over GaN. These include (1) the much larger value of α (~ 42 in AlN in the $\vec{E} \perp \vec{c}$ configuration versus ~ 8.9 in GaN in both polarization configurations),²¹ (2) smaller exciton Bohr radii (~ 12 Å in AlN versus ~ 27 Å in GaN due to the differences in the effective masses and dielectric constants),^{24,25} and (3) stronger ionic bonding between Al–N over Ga–N.

A comparison between heteroepilayers and homoepilayers has also been carried out and the results are shown in Fig. 3. In the AlN homoepilayer, emission lines at 6.03, 5.92, and 5.81 eV are due to the recombination of the free exciton and its 1LO and 2LO phonon replica, while the dominant emission line at 6.01 eV is associated with the donor-bound exciton (I_2).²⁶ The exciton-phonon coupling constant is found to be slightly larger in heteroepilayers ($S=0.11$ for heteroepilayer versus 0.09 for homoepilayer). A previous study has indicated that the emission intensities of phonon replica lines in GaN are lower in epilayers containing higher density of impurities.²⁷ Due to the possible diffusion of residual impurities in the AlN bulk substrate to the epilayer; our homoepilayers also contain higher density of unintentional donors than the heteroepilayers, as corroborated by the fact that the I_2 emission is dominant in homoepilayers [Fig. 3(b)]. In materials with high impurity concentrations, the scattering of exciton-polariton may be enhanced by impurity or related defects. Such scattering may assist in momentum transfer, and hence recombination becomes possible without the participation of phonons, which reduces the number of phonons involved, therefore weakening the coupling. Reduced efficiency of phonon assisted exciton emissions due to the

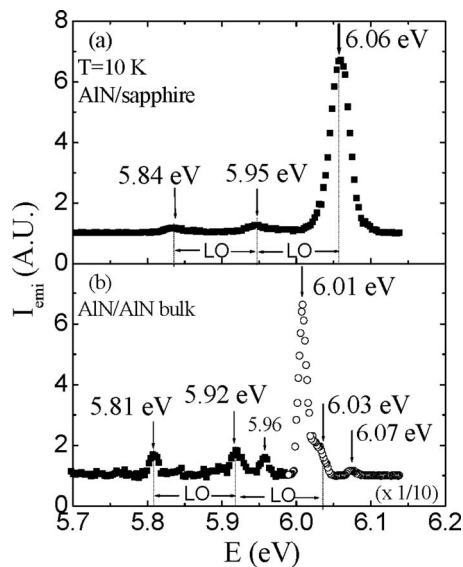


FIG. 3. Low temperature (10 K) PL spectra of (a) an AlN heteroepilayer grown on sapphire and (b) an AlN homoepilayer on grown on bulk AlN substrate.

enhanced scattering by defects has also been observed in *p*-type GaN.²⁸ Moreover, a previous observation of strong LO phonon replica emission lines relative to the zero-phonon line in Ga-face GaN epilayers (lower defect density) and almost no phonon replica in *N*-face GaN (higher defect density) is consistent with this argument because different polarities affect the growth modes and therefore the incorporation of defects.²⁹

In summary, exciton-phonon interactions in AlN have been investigated and it has been found that the coupling constant in AlN depends on the polarization configuration, and are 0.78 and 0.11 for the $\vec{E} \perp \vec{c}$ and $\vec{E} \parallel \vec{c}$ configuration, respectively. Moreover, the coupling constant is larger in AlN than in GaN. The larger hole to electron effective mass ratio in AlN, especially in the $\vec{E} \perp \vec{c}$ polarization configuration, is one of the predominant factors that accounts for the observed strong exciton-LO phonon coupling strength in AlN. The strong carrier-phonon interaction in AlN may be exploited to maximize the benefits of phonon-assisted transitions in AlN based optoelectronic devices.

This research is supported by DOE (Grant No. DE-FG02-09ER46552). J.Y.L. and H.X.J. gratefully acknowledge the support of the Linda Whitacre and Edward Whitacre endowed chair positions through the AT & T Foundation.

- ¹J. Li, K. B. Nam, M. L. Nakarmi, J. Y. Lin, and H. X. Jiang, *Appl. Phys. Lett.* **81**, 3365 (2002).
- ²K. B. Nam, J. Li, M. L. Nakarmi, J. Y. Lin, and H. X. Jiang, *Appl. Phys. Lett.* **82**, 1694 (2003).
- ³J. Li, K. B. Nam, M. L. Nakarmi, J. Y. Lin, H. X. Jiang, P. Carrier, and S. H. Wei, *Appl. Phys. Lett.* **83**, 5163 (2003).
- ⁴M. Horita, J. Suda, and T. Kimoto, *Appl. Phys. Lett.* **89**, 112117 (2006).
- ⁵Y. Taniyasu, M. Kasu, and T. Makomoto, *Nature (London)* **441**, 325 (2006).
- ⁶J. Li, Z. Y. Fan, R. Dahal, M. L. Nakarmi, J. Y. Lin, and H. X. Jiang, *Appl. Phys. Lett.* **89**, 213510 (2006).
- ⁷R. Dahal, T. M. Al Tahtamouni, Z. Y. Fan, J. Y. Lin, and H. X. Jiang, *Appl. Phys. Lett.* **90**, 263505 (2007).
- ⁸A. BenMoussa, J. F. Hochedez, R. Dahal, J. Li, J. Y. Lin, H. X. Jiang, A. Soltani, and J.-C. De Jaeger, *Appl. Phys. Lett.* **92**, 022108 (2008).
- ⁹B. Pantha, R. Dahal, M. L. Nakarmi, N. Nepal, J. Y. Lin, and H. X. Jiang, *Appl. Phys. Lett.* **90**, 241101 (2007).
- ¹⁰X. B. Zhang, T. Taliercio, S. Kolliakos, and P. Lefebvre, *J. Phys.: Condens. Matter* **13**, 7053 (2001).
- ¹¹L. Bergman, M. Dutta, C. Balkas, R. F. Davis, J. A. Christman, D. Alexson, and R. J. Nemanich, *J. Appl. Phys.* **85**, 3535 (1999).
- ¹²G. Popovici, G. Y. Xu, A. Botchkarev, W. Kim, H. Tang, A. Salvador, H. Morkoc, R. Strange, and J. O. White, *J. Appl. Phys.* **82**, 4020 (1997).
- ¹³D. C. Reynolds, D. C. Look, B. Jogai, and R. J. Molnar, *Solid State Commun.* **108**, 49 (1998).
- ¹⁴M. Smith, J. Y. Lin, H. X. Jiang, A. Khan, Q. Chen, A. Salvador, A. Botchkarev, W. Kim, and H. Morkoc, *Appl. Phys. Lett.* **70**, 2882 (1997).
- ¹⁵N. Nepal, K. B. Nam, M. L. Nakarmi, J. Y. Lin, H. X. Jiang, J. M. Zavada, and R. G. Wilson, *Appl. Phys. Lett.* **84**, 1090 (2004).
- ¹⁶K. B. Nam, J. Li, M. L. Nakarmi, J. Y. Lin, and H. X. Jiang, *Appl. Phys. Lett.* **84**, 5264 (2004).
- ¹⁷B. Di Bartolo and R. Powell, *Phonons and Resonances in Solids* (Wiley, New York, 1976), Chap. 10.
- ¹⁸K. W. Böer, *Survey of Semiconductor Physics* (Van Nostrand Reinhold, New York, 1990), Chap. 20.
- ¹⁹H. Zhao and H. Kalt, *Phys. Rev. B* **68**, 125309 (2003).
- ²⁰H. L. Malm and R. R. Haering, *Can. J. Phys.* **49**, 2970 (1971).
- ²¹D. L. Dexter and R. S. Knox, *Excitons* (Interscience, New York, 1965), pp. 52–54.
- ²²M. Suzuki, T. Uenoyama, and A. Yanase, *Phys. Rev. B* **52**, 8132 (1995).
- ²³W. Liu, M. F. Li, S. J. Xu, K. Uchida, and K. Matsumoto, *Semicond. Sci. Technol.* **13**, 769 (1998).
- ²⁴G. Steude, B. K. Meyer, A. Göldner, A. Hoffmann, F. Bertram, and J. Christen, *Appl. Phys. Lett.* **74**, 2456 (1999).
- ²⁵H. Morkoc, *Nitride Semiconductors and Devices* (Springer, New York, 1999).
- ²⁶A. Sedhain, N. Nepal, M. L. Nakarmi, T. M. Al Tahtamouni, J. Y. Lin, H. X. Jiang, Z. Gu, and J. H. Edgar, *Appl. Phys. Lett.* **93**, 041905 (2008).
- ²⁷I. A. Buyanova, J. P. Bergman, B. Monemar, H. Amano, and I. Akasaki, *Mater. Sci. Eng., B* **50**, 130 (1997).
- ²⁸H. Y. An, O. H. Cha, J. H. Kim, G. M. Yang, K. Y. Lim, E. K. Suh, and H. J. Lee, *J. Appl. Phys.* **85**, 2888 (1999).
- ²⁹M. Sumiya, T. Ohnishi, M. Tanaka, A. Ohtomo, M. Kawasaki, M. Yoshimoto, H. Koinuma, K. Ohtsuka, and S. Fuke, *Mater. Res. Soc. Symp. Proc.* **537**, G623 (1999).